

First- and last-passage Monte Carlo algorithms for the charge density distribution on a conducting surface

James A. Given,^{1,*} Chi-Ok Hwang,^{2,†} and Michael Mascagni^{3,‡}¹Naval Research Laboratory, 4555 Overlook Avenue SW, Washington, DC 20375²Innovative Technology Center for Radiation Safety, Hanyang University, HIT Building, 17 Haedang-Dong, Sungdong-Gu, Seoul 133-791, Korea³Department of Computer Science and School of Computational Science and Information Technology, Florida State University, Tallahassee, Florida 32306

(Received 7 August 2002; published 22 November 2002)

Recent research shows that Monte Carlo diffusion methods are often the most efficient algorithms for solving certain elliptic boundary value problems. In this paper, we extend this research by providing two efficient algorithms based on the concept of “last-passage diffusion.” These algorithms are qualitatively compared with each other (and with the best first-passage diffusion algorithm) in solving the classical problem of computing the charge distribution on a conducting disk held at unit voltage. All three algorithms show detailed agreement with the known analytic solution to this problem.

DOI: 10.1103/PhysRevE.66.056704

PACS number(s): 45.10.-b, 02.70.Rr, 41.20.-q

I. INTRODUCTION

In recent times, there has been very substantial progress in the development of diffusion Monte Carlo methods for solving problems in the domains of materials science and biophysics [1–4]. Both these applications frequently involve problems that require solving the Laplace equation, or another elliptic partial differential equation, in a multiphase domain where the phase boundary is extensive, convoluted, and singular; i.e., containing corners, cusps, and edges.

A recent work has provided the most efficient algorithms yet devised for calculating bulk parameters in such systems, the Green’s-function first-passage algorithms [1,2,4,5]. In particular, efficient algorithms of this kind now exist for the calculation of the permeability of packed beds, the conductivity of two-phase composites, and the diffusion-limited reaction rate for systems involving protein-ligand binding.

But much remains to be done. A large fraction of the advances made in recent decades by theorists of Brownian motion have apparently not yet been incorporated into efficient numerical algorithms. In particular, the concepts of last passage [6], local time, and speed measure [7], which are of central importance in probability, do not yet seem to be incorporated into efficient algorithms.

In this paper, we introduce the first efficient algorithms based on the concept of last passage. These methods involve Brownian motion “reversed in time,” in a sense which has been made precise [6]. In these algorithms, diffusing particles leave the sites at which they are absorbed and diffuse to the places where they are created. Such algorithms have an advantage over first-passage diffusion algorithms for at least four different types of problems:

(1) Problems in which the detailed distribution of absorption sites is important. First-passage methods do provide this distribution; however, they provide the distribution of absorption sites according to naive importance sampling. The distribution is estimated over the entire surface, this does not provide efficient solutions for problems in which one requires the detailed surface charge distribution in a localized patch, or on a line segment, especially if the total surface charge density in the area of interest is small.

(2) Problems such as binding-site problems in which the absorption sites are highly localized and make up a very small fraction of the interface. Here it is more efficient for diffusing particles to start at the absorption sites than it is for them to search for absorption sites starting from the outside.

(3) Problems in which multiple absorbing surfaces are placed in close proximity to one another. These problems effectively involve the calculation of a mutual capacitance matrix. First-passage methods cannot address these problems.

(4) Problems in which the interface involves singularities, i.e., folds, cusps, and corners. Absorption points collect at these singularities. Last-passage methods locate and map out this part of the total absorption surface very efficiently.

The present paper addresses the first set of problems described above. In particular, we develop and explore a different set of last-passage algorithms for computing the charge distribution on a conducting surface. We apply them to a specific exactly solvable problem, namely, the calculation of the surface charge density on a circular conducting disk held at unit potential.

This paper is organized as follows. In Sec. II, we develop the first-passage Monte Carlo algorithm for computing the charge density on a conducting surface. In Sec. III, we develop a class of last-passage diffusion algorithms for computing electrostatic properties of a conducting surface. In Sec. IV, a class of “edge-distribution” algorithms is developed as a general method for making last-passage algorithms more efficient. In Sec. V, these three classes of algorithms for surface charge density are employed to calculate the electro-

*Email address: JAGiven137@aol.com

†Email address: chwang@itrs.hanyang.ac.kr

‡Email address: mascagni@cs.fsu.edu;

URL: <http://www.cs.fsu.edu/~mascagni>

static properties of a conducting circular disk. This example is used to exhibit the relative advantages and disadvantages of each class of algorithms. Section VI provides our conclusions.

II. THE FIRST-PASSAGE ALGORITHM FOR THE CHARGE DENSITY ON A CONDUCTOR

In this section, we review the isomorphism, provided by probabilistic potential theory [8,9], between the electrostatic Dirichlet problem on a conducting surface and the corresponding Brownian motion expectation.

Consider the electrostatic Dirichlet problem for the exterior Laplace equation in a volume Ω , with boundary $\partial\Omega$. Let $\phi(\mathbf{x})$ be the electrostatic potential, satisfying the Laplace equation:

$$\Delta \phi(\mathbf{x}) = 0, \quad \mathbf{x} \in \Omega, \quad (1)$$

with the boundary conditions,

$$\phi(\mathbf{x}) = 1, \quad \mathbf{x} \in \partial\Omega, \quad (2)$$

and

$$\phi(\mathbf{x}) = 0 \quad \text{as} \quad \mathbf{x} \rightarrow \infty. \quad (3)$$

For understanding the Brownian motion expectation, it is convenient to think in terms of a diffusion problem, as Brownian motion is the microscopic manifestation of diffusion. Thus the isomorphic diffusion problem is described as follows: define the function $\bar{\phi}(\mathbf{x})$ to be the probability density associated with a diffusing (Brownian) particle initiating at point \mathbf{x} and diffusing indefinitely far away without ever making contact with the surface $\partial\Omega$. The function $\bar{\phi}(\mathbf{x})$ obeys the sphere averaging property; thus it is a harmonic function. In addition, it obeys the boundary conditions

$$\bar{\phi}(\mathbf{x}) = 0, \quad \mathbf{x} \in \partial\Omega, \quad (4)$$

and

$$\bar{\phi}(\mathbf{x}) = 1 \quad \text{as} \quad \mathbf{x} \rightarrow \infty. \quad (5)$$

The uniqueness of solutions to the Laplace equation thus implies that

$$\bar{\phi}(\mathbf{x}) = 1 - \phi(\mathbf{x}). \quad (6)$$

A different isomorphism between an electrostatic problem and a diffusion problem provides a practical first-passage algorithm for the surface charge distribution on a conductor held at a nonzero potential with respect to the point at infinity [3]. The principle of inversion with respect to a sphere in electrostatic problems shows that such a potential is equivalent to a large point charge (or equivalently, a source of Brownian or diffusing particles) placed far away from the conducting object. Brownian particles leaving such a point source will make first-passage at a set of uniformly spaced positions on a sphere (usually termed a “launch sphere,” see Fig. 1) surrounding the conducting/absorbing object. (Note

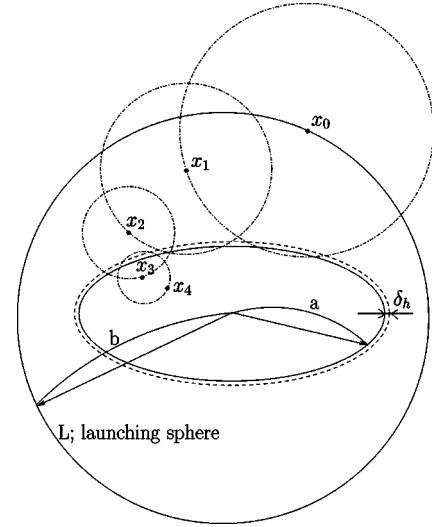


FIG. 1. A schematic view that illustrates an absorbed series of first-passage jumps in a circular disk of radius a using “walk on spheres” (WOS) [10,13–16]. In WOS, the boundary is thickened by δ_h . When a Brownian particle is initiated with uniform probability from the launching sphere L of radius b , and enters this δ_h absorption layer, the Brownian trajectory is terminated.

that this fact is independent of the placement of the launch sphere; in particular, of the position of its center.) Thus one can efficiently simulate the equivalent diffusion problem by initiating Brownian particles at uniformly distributed first passage positions on the launch sphere. These Brownian particles will ultimately either make first passage on the absorbing object or diffuse to infinity in a way that is well defined. The location of the first-passage positions of the Brownian particles will thus have a distribution identical to that of the surface charge density in the above electrostatic problem.

III. A LAST-PASSAGE ALGORITHM FOR SURFACE CHARGE DENSITY

In this section, we introduce a last-passage algorithm that allows one to efficiently calculate the charge density at a general point on a conducting surface by using the Brownian (diffusing) paths that initiate at that point.

One can utilize the first isomorphism developed in Sec. VI section between electrostatic problems and diffusion problems to obtain a formula for the electrostatic potential $V(\mathbf{x} + \epsilon)$, very near the point \mathbf{x} on the conducting surface [10]:

$$V(\mathbf{x} + \epsilon) = \int_{\partial\Omega_y} d^2\mathbf{y} g(\mathbf{x} + \epsilon, \mathbf{y}) p(\mathbf{y}, \infty). \quad (7)$$

Here, $g(\mathbf{x} + \epsilon, \mathbf{y})$ is the Laplacian Green’s function associated with Dirichlet boundary conditions on the region $\partial\Omega_y$ (see Fig. 2). In particular, $g(\mathbf{x} + \epsilon, \mathbf{y})$ is the probability density associated with a diffusing particle initiating at the point $\mathbf{x} + \epsilon$ and making first passage on the surface $\partial\Omega_y$ at the point \mathbf{y} . Also, $p(\mathbf{y}, \infty)$ is the probability density associated with a diffusing particle initiating at the point \mathbf{y} on the upper first-

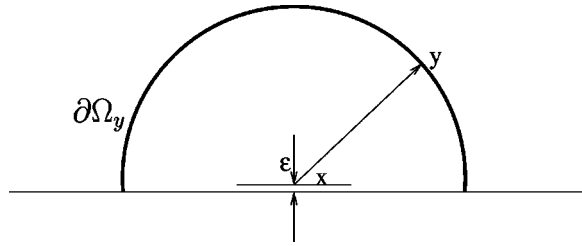


FIG. 2. A conducting surface is shown edge on; $g(\mathbf{x} + \epsilon, \mathbf{y})$ is the probability density associated with a Brownian particle initiating at the point $\mathbf{x} + \epsilon$ and making first-passage on the surface $\partial\Omega_y$ at the point \mathbf{y} .

passage surface and diffusing to infinity without ever returning to the lower first-passage surface.

Thus, Eq. (7) represents the electrostatic potential $V(\mathbf{x} + \epsilon)$ as the probability density associated with a diffusing particle initiating at the point $\mathbf{x} + \epsilon$ near a conducting surface, and diffusing without ever contacting the conducting surface. This is consistent with the first isomorphism presented in Sec. II. We note an essential fact about the integrand in Eq. (7); the first factor is analytically simple, but it depends on the quantity ϵ ; the second factor is very complicated, but it is independent of ϵ .

Gauss' law gives the surface charge density $\sigma(\mathbf{x})$ on a conductor in terms of the formula [11]

$$\sigma(\mathbf{x}) = - \frac{1}{4\pi} \frac{d}{d\epsilon} \Big|_{\epsilon=0} V(\mathbf{x} + \epsilon). \quad (8)$$

Inserting Eq. (7) for $V(\mathbf{x} + \epsilon)$, this becomes

$$\sigma(\mathbf{x}) = \frac{1}{4\pi} \int_{\partial\Omega_y} d^2\mathbf{y} G(\mathbf{x}, \mathbf{y}) p(\mathbf{y}, \infty), \quad (9)$$

where

$$G(\mathbf{x}, \mathbf{y}) = \frac{d}{d\epsilon} \Big|_{\epsilon=0} g(\mathbf{x} + \epsilon, \mathbf{y}). \quad (10)$$

The function $G(\mathbf{x}, \mathbf{y})$ is the Laplacian Green's function for a point dipole centered on the conducting surface at point \mathbf{x} and normal to the surface (see Fig. 3).

For a flat conducting surface, this dipole Green's function is readily shown to be given by

$$G(\mathbf{x}, \mathbf{y}) = \frac{3}{2\pi} \frac{\cos \theta}{a^3}, \quad (11)$$

where θ is the angle between the vectors x and y , and a is the radius of the absorbing sphere. Substituting Eq. (11) into Eq. (9) gives the formula

$$\sigma(\mathbf{x}) = \frac{3}{8\pi^2} \int_{\partial\Omega_y} dS \frac{\cos \theta}{a^3} p(\mathbf{y}, \infty). \quad (12)$$

The last-passage method obtains the charge density on the circular plate at the point \mathbf{x} as follows. N diffusing particles

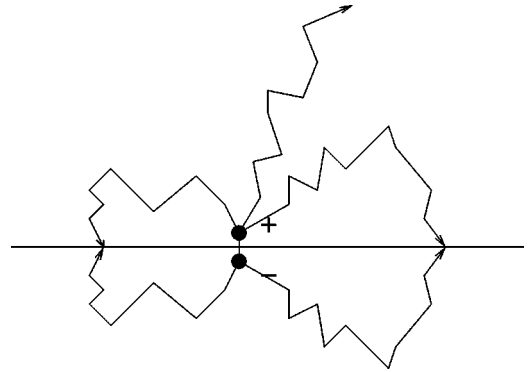


FIG. 3. The Green's function for a point dipole oriented normally to an absorbing surface is a generating function for Brownian trajectories that leave the absorbing surface and never return. The effect of trajectories that leave and do return is zero; they cancel out in pairs.

are initiated at points selected randomly with density $\cos \theta dS$ on the surface of a hemisphere surrounding the point \mathbf{x} . They diffuse until they either hit the conducting disk or diffuse far away. The surface charge density at the point \mathbf{x} is then given by

$$\sigma(\mathbf{x}) = \frac{3}{16a} \frac{N_1}{N}, \quad (13)$$

where N_1 is the number of diffusing particles that diffuse to infinity.

IV. ON THE USE OF EDGE DISTRIBUTIONS IN THE IMPLEMENTATION OF LAST-PASSAGE ALGORITHMS

In this section, we provide an introduction to the concept of "edge distribution." We explain the use of this concept in the context of last-passage distributions.

The benefits of last-passage distribution have already been explained in the Introduction. Nonetheless, algorithms based on the first-passage distribution have one natural advantage; they incorporate importance sampling, i.e., they take into account the fact that corners and edges accumulate charge. Indeed, they support charge singularities. For a large class of important problems, one can divide the surface of the absorbing object into two subsets:

(a) The corners and edges.

(b) The remainder of the surface, assumed smooth and singularity free. The edge distribution method provides a Metropolis-like method, i.e., an approximate importance sampling method with correction, for this class of problems. In particular, problems in which the absorbing surface consists of a number of polygonal faces, either flat or curved, joined together at their corners and edges, can be treated in this manner.

First, points are chosen according to an approximate probability density defined as follows: Each polygonal face is assumed to have constant and equal charge density on the portion of it that is away from all edges. The charge density in a strip adjoining each edge is taken to have a form containing an (integrable) singularity [11]

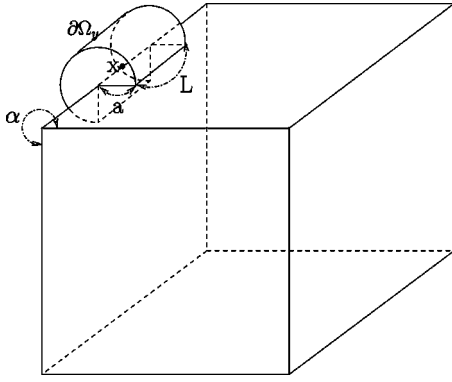


FIG. 4. A three-quarter cylinder of radius a and length L on the edge of a cube is shown. Here $\partial\Omega_y$ is a chopped cylindrical surface that intersects the pair of absorbing surfaces meeting at angle α .

$$\sigma = C \left[\frac{\delta}{\delta_0} \right]^{1-\pi/\alpha}. \quad (14)$$

Here, δ is the distance from the center of the polygonal face, and α is the angle between the two faces that meet at the edge nearest to the sample point. The constants C and δ_0 are chosen to make the charge densities at the center of each polygon equal. Specifically, this strip is sampled with a local density given by

$$\sigma(\mathbf{x}, \delta) = \delta^{\pi/\alpha-1} \sigma_e(\mathbf{x}). \quad (15)$$

The edge distribution $\sigma_e(\mathbf{x})$ for an edge of the conductor can be determined by calculating the charge distribution for a single curve parallel to the edge, but near to it, by using the last-passage method, and then using the above scaling law. Once the edge distribution for a given edge is determined, it allows rapid estimation of the surface charge density at any point close to that edge, again, by using the scaling law. No additional Monte Carlo simulation is needed for such estimations.

The edge distribution has a natural probabilistic interpretation. It is the (rescaled) probability density that a diffusing particle makes last passage on the edge point \mathbf{x} . This distribution can be calculated either by simulation or by application of the general formula from Eq. (15). The point is that this one-dimensional distribution needs to be calculated only once for each edge on each absorbing object in a problem. An extension of Eq. (9) for $\sigma(\mathbf{x})$ gives a formula for the edge distribution:

$$\sigma_e(\mathbf{x}) = \frac{1}{4\pi} \lim_{\delta \rightarrow 0} \delta^{1-\pi/\alpha} \int_{y \in \partial\Omega_y} d^2\mathbf{y} G(\mathbf{x}, \mathbf{y}) p(\mathbf{y}, \infty). \quad (16)$$

Here $\partial\Omega_y$ is a cylindrical surface that intersects the pair of absorbing surfaces meeting at angle α (as an example, for a cube, see Fig. 4).

The power of the edge distribution method is twofold. First, it provides an (approximate) importance sampling technique that is free of the singularities associated with edges and corners. Second, the edge distribution method will place most of its sample points very near the edges due to the

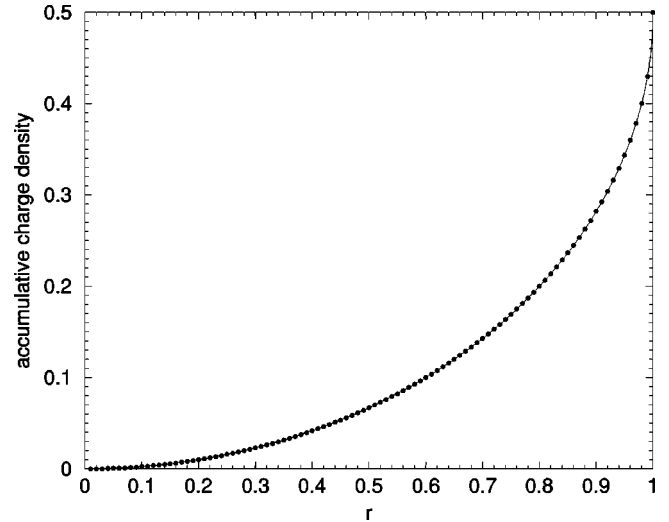


FIG. 5. Cumulative charge density at r from the center of a unit two-dimensional disk in three dimensions.

fact that this is where surface charge collects. The charge distribution at these points can be calculated from Eq. (15) without any additional Monte Carlo simulation.

In this paper, we only study a single problem; one in which the edge distribution reduces to a constant. But even this problem will serve to demonstrate the computational advantages of this method.

V. THE CHARGE DISTRIBUTION ON A CONDUCTING CIRCULAR PLATE

In this section, we use a classical problem of electrostatics, the problem of the circular conducting plate held at unit potential, as a laboratory to explore the relative efficiencies of the three algorithms discussed in this paper. We explore both the problem of calculating the charge distribution in a localized region and the problem of calculating the total charge on the conducting plate, i.e., the capacitance.

The conductor we consider is a thin two-dimensional circular disk lying in the x - y plane in three dimensions. When the potential of the disk is unity with respect to infinity, the charge density is given analytically [12] by

$$\sigma(r) = \frac{1}{4\pi a^2} \frac{1}{\sqrt{1-r^2/a^2}}, \quad (17)$$

where a is the radius of the disk and r is the radial distance from the center of the disk.

One can assess the quality of the charge density distribution obtained by using the first-passage algorithm by studying the radial cumulative charge density distribution. In Fig. 5, the cumulative charge density at r from the center of a unit two-dimensional disk in three dimensions is shown. For the convergence of the cumulative charge density, Fig. 6 shows the relative error of cumulative charge density at r , from the center of a unit two-dimensional disk in three dimensions. Also, Fig. 7 shows the averaged relative errors of the cumulative charge density along the radial direction with respect

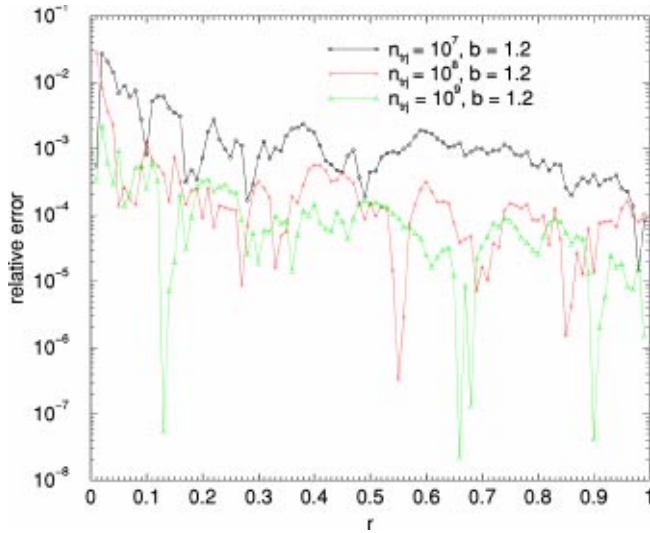


FIG. 6. Relative error of the cumulative charge density at r from the center of a unit two-dimensional disk in three dimensions. This shows the convergence of the cumulative charge density. Here, n_{trj} is the number of Brownian trajectories and b the radius of the launch sphere.

to the number of random walks. In Fig. 8, it is shown that the smaller launch sphere size is the better. The reason is that when the launch sphere radius is smaller, the probability of making contact of the disk is higher, so that we have more samplings. Figure 9 shows that the launch sphere center location does not matter, provided that the launch sphere encloses the conducting object completely. These results support the derivation of the first-passage algorithm presented in Sec. II.

The last-passage algorithm is used to calculate the charge density on the conducting disk by performing a simulation

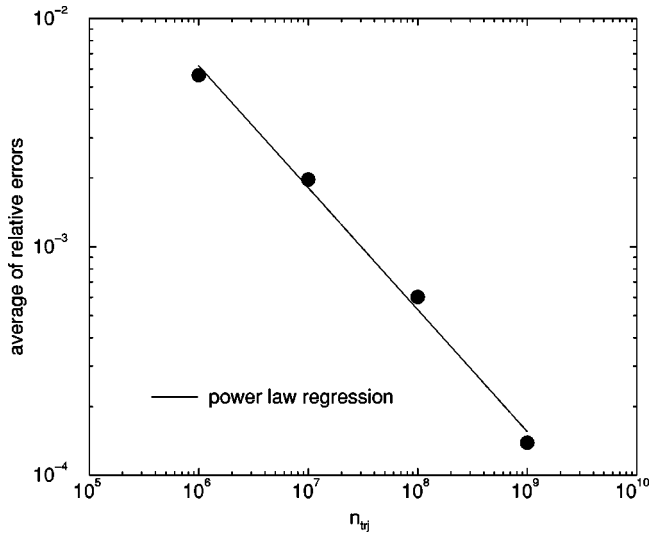


FIG. 7. The averaged relative error of the cumulative charge density along the radial direction with respect to the number of random walks. This shows the convergence of the cumulative charge density. The slope (convergence rate) shows the usual convergence rate of Monte Carlo simulations, about 0.5. Here, n_{trj} is the number of Brownian trajectories.

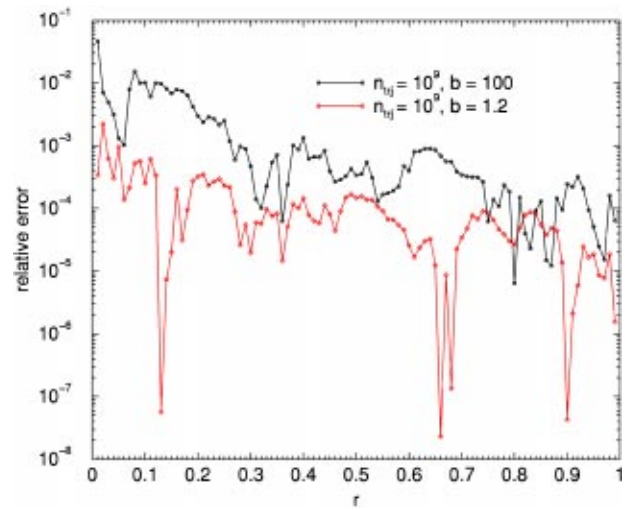


FIG. 8. The relative error of cumulative charge density at r from the center of a unit two-dimensional disk in three dimensions. This shows that the smaller launch sphere size, the better it is. Here, n_{trj} is the number of Brownian trajectories and b is the radius of the launch sphere.

based on Eq. (12). To calculate the charge density at a point r , starting points are chosen at random positions, \mathbf{y} , on a hemisphere centered at the point r (see Fig. 10). Each point is weighted by the quantity $G(r, \mathbf{y})$. The path of a Brownian particle is simulated until it either touches the sphere again or diffuses to infinity. The charge density at point r , $\sigma(r)$, is given as the average of the quantity $G(r, \mathbf{y})$ over the set of paths that *do not* return to the disk.

In this illustrative circular disk problem, we know the analytic potential at a distance from the disk so that we can use this analytic potential function as the probability of going back to the disk. In a simulation with 10^6 Brownian trajectories of Fig. 11, we use the analytic potential function to

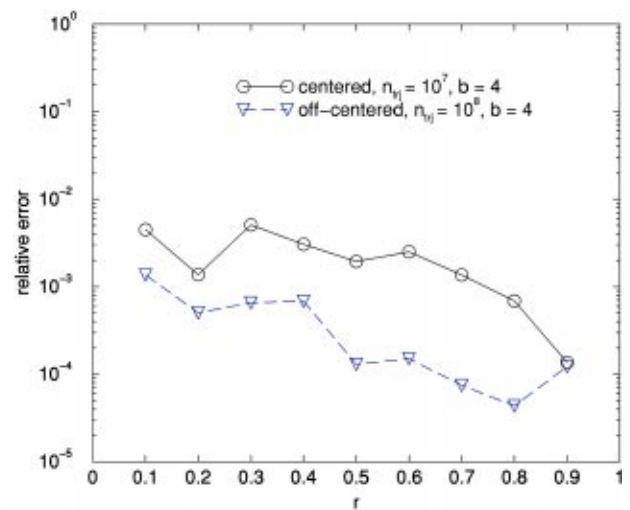
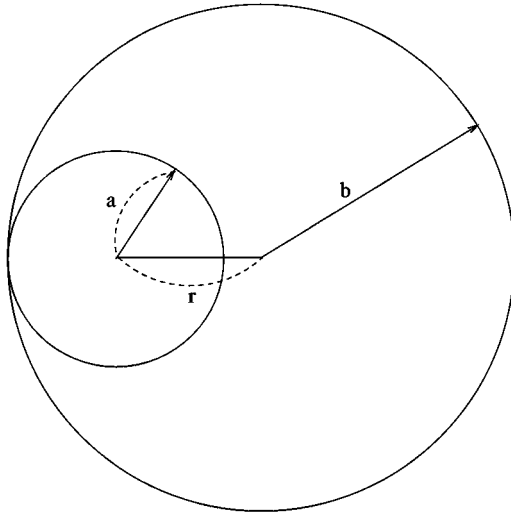


FIG. 9. The relative error of cumulative charge density at r from the center of a unit two-dimensional disk in three dimensions. This shows that the launch sphere center location does not matter. The center of the disk is $(1, 0.5, 0.75)$. Here, n_{trj} is the number of Brownian trajectories and b the radius of the launch sphere.

From the top



From the side

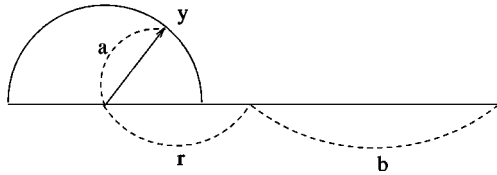


FIG. 10. A schematic top view and side view of a two-dimensional circular disk of radius b in three dimensions. This illustrates the charge density calculation at r ; for a last passage point y , a hemisphere of radius a is drawn.

decide whether the Brownian particle goes back to the disk or not. σ_0 is the charge density at the center of the disk. Second, in Fig. 12 we use another simulation to get the charge density at distance r from the center. We use a “walk

charge density on a circular disk

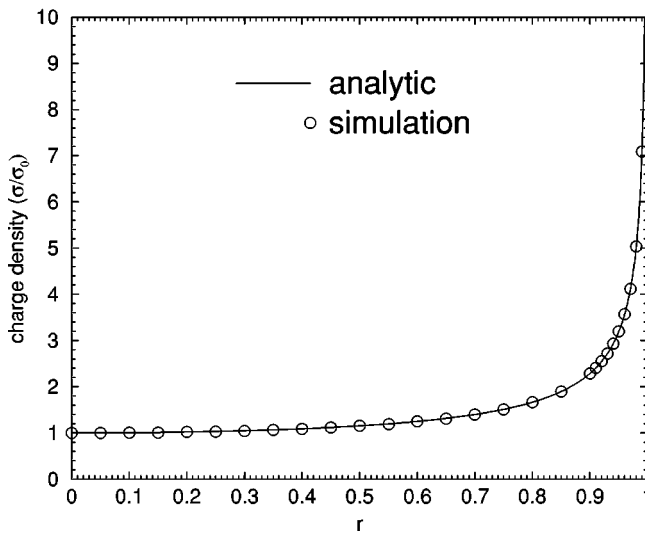


FIG. 11. The charge density at r from the center of a unit two-dimensional disk in three dimensions. σ_0 is the charge density at the center of the disk. We use the analytic potential function to decide whether the Brownian particle goes back to the disk or not.

charge density on a circular disk

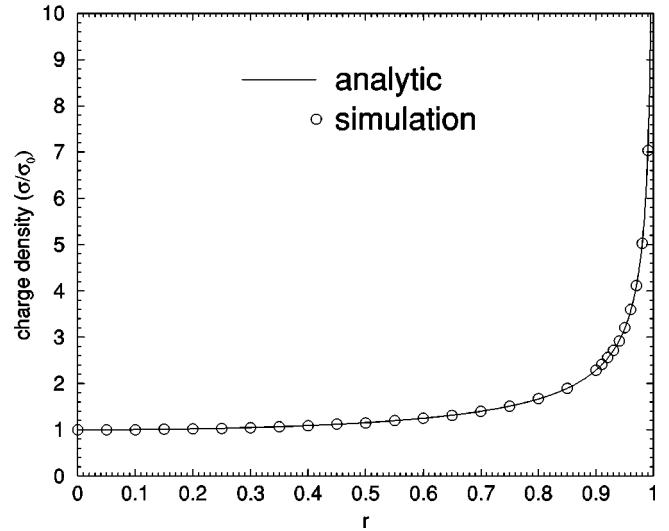


FIG. 12. The charge density at r from the center of a unit two-dimensional disk in three dimensions. σ_0 is the charge density at the center of the disk. We use a WOS simulation to decide whether the Brownian particle goes back to the disk or not.

on spheres” (WOS) simulation [10,13–16] to decide whether the Brownian particle goes back to the disk or not. In general, there will be no known analytic potential so that we will rely on WOS (see Fig. 1). In Table I, we show that it is possible to estimate the charge density accurately at points very close to the edge singularity.

We use a Monte Carlo integration method for computing the total charge on the disk, with the importance sampling

$$\int_0^1 2\sqrt{(1-r)}f(r)d(-\sqrt{1-r}). \tag{18}$$

To remove the singularity at the edges [11], we introduce the term $\sqrt{(1-r)}$. Here, $f(r)$ is the radial charge distribution on the unit circular disk including the charge singularity term $1/\sqrt{1-r}$, and r the radial distance from its center. Random positions are chosen via the random variable $1-\eta^2$, where η is uniform in $[0,1)$.

This method gives the result 0.50094 for the total charge on one side of the disk, when 10^4 sampling positions are

TABLE I. The charge density at points very close to the edge of the circular disk. The values of $r=0.99$, 10^8 Brownian trajectories, and a 10^{-7} unit-wide absorption layer are used with 10^9 trajectories, and a 10^{-12} unit-wide absorption layer is used for $r=0.999$. Here, r is the radial distance from the center of a unit two-dimensional disk in three dimensions. This is how one can estimate the charge density at points very close to a singularity using last-passage methods.

Position (r)	Analytic	Simulation
0.99	0.5641	0.5638
0.999	1.7799	1.7820

TABLE II. The charge density at points very close to the edge of the circular disk using the edge distribution. Here, r is the radial distance from the center of a unit two-dimensional disk in three dimensions. The third column shows charge density computed using edge distribution, and the fourth column shows this with the first correction term.

Position (r)	Analytic	Edge distribution	
		Edge distribution	with first correction
0.9	0.18256324	0.177940636	0.182389152
0.99	0.564109739	0.562697698	0.564104442
0.999	1.77985138	1.77940636	1.77985121
0.9999	5.62711766	5.62697698	5.62711765
0.99999	17.7941081	17.7940636	17.7941081
0.999999	56.2697838	56.2697698	56.2697838
0.9999999	177.940640	177.940636	177.940640
0.99999999	562.697698	562.697696	562.697698
0.999999999	1779.40638	1779.40638	1779.40638

used, with 10^4 Brownian trajectories for each sampling position. Here the first-passage method is much faster and easier to implement than this last-passage algorithm.

For the circular plate, the edge distribution $\sigma_e(x)$ is constant because the edge singularity is the same at each point near the edge of the disk, by symmetry. It is known that the charge density on a circular disk is given analytically by Eq. (17). Letting $r = a - x$ and $z = r/a$,

$$\sigma(z) = \frac{1}{4\pi a^2} \frac{1}{\sqrt{2z}} (1 - z/2)^{-1/2}, \quad (19)$$

after Taylor expansion,

$$\sigma_e = \frac{1}{4\sqrt{2}\pi a^2}, \quad (20)$$

and the first correction term will be

$$\frac{1}{16\sqrt{2}\pi a^2} z^{1/2}. \quad (21)$$

In Table II, we show that it is possible to estimate the charge density very close to a singularity using the edge distribution concept. The third column shows charge density computed using edge distribution, and the fourth column

with the first correction term. In general, the edge distribution will not be constant; however, using the natural probabilistic interpretation, we can obtain the edge distribution along finite-sized edges. We intend to publish these results in a follow-on paper.

VI. DISCUSSION AND CONCLUSIONS

In this paper, we have presented three Monte Carlo methods for computing the charge density on a conductor when the conductor is held at a potential V_0 with respect to infinity. The first method has extended the first-passage algorithm for the capacitance calculation of an arbitrarily shaped conducting object. It turns out that the probability distribution of the absorption locations of the first-passage capacitance calculation give the charge distribution on the conducting object, regardless of the centers and sizes of the launch sphere if the launch sphere encloses the conducting object completely. The second Monte Carlo method utilizes the last-passage concept. The last-passage method stems from the isomorphism between the electrostatic potential and the probability of a Brownian path going to infinity without returning to the conductor. The third method also uses the last-passage concept, enhanced by using the edge distribution to provide approximate importance sampling. This allows fast calculation of charge density near the edges of a conductor.

Each method has advantages and disadvantages. The first-passage method is good for calculating the capacitance of the conducting object, for obtaining the global charge density distribution on a conducting object, or for the total charge density on a surface region of a conducting object. Using the first-passage algorithm to estimate the charge density at a specific point, we need postprocessing. We must calculate the derivative of the charge distribution at the point. This postprocessing is rapid for symmetric objects such as the flat disk, but for objects of general shape, it is more problematic. Therefore, to estimate the charge density at a specific point not too close to the edges or corners of a conducting object, the basic last-passage method is more suitable. For points very close to edges or corners of a conducting object, the edge distribution method will provide the most accurate estimates.

ACKNOWLEDGMENTS

We wish to acknowledge the financial support of the Accelerated Strategic Computing Initiative (ASCI). Also, we give special thanks to the Innovative Technology Center for Radiation Safety (iTRS), the Hanyang University, Seoul, Korea, for partial support of this work.

- [1] C.-O. Hwang, J.A. Given, and M. Mascagni, *J. Comput. Phys.* **174**, 925 (2001).
 [2] C.-O. Hwang, J.A. Given, and M. Mascagni, *Phys. Fluids* **12**, 1699 (2000).
 [3] M.L. Mansfield, J.F. Douglas, and E.J. Garboczi, *Phys. Rev. E* **64**, 061401 (2001).

- [4] C.-O. Hwang, J.A. Given, and M. Mascagni, *Monte Carlo Met.* **7**, 213 (2001).
 [5] J.A. Given, M. Mascagni, and C.-O. Hwang, *Lect. Notes Comput. Sci.* **2179**, 46 (2001).
 [6] K.L. Chung, *Green, Brown, and Probability* (World Scientific, Singapore, 1995).

- [7] A.N. Borodin and P. Salminen, *Handbook of Brownian Motion: Facts and Formulae (Probability and Its Applications)* (Springer-Verlag, Berlin, 1996).
- [8] M. Freidlin, *Functional Integration and Partial Differential Equations* (Princeton University Press, Princeton, NJ, 1985).
- [9] K.L. Chung and Z. Zhao, *From Brownian Motion to Schrödinger's Equation* (Springer-Verlag, Berlin, 1995).
- [10] M.E. Müller, *Ann. Math. Stat.* **27**, 569 (1956).
- [11] J.D. Jackson, *Classical Electrodynamics* (Wiley, New York, 1975).
- [12] W.R. Smythe, *Static and Dynamic Electricity* (McGraw-Hill, New York, 1939).
- [13] A. Haji-Sheikh and E.M. Sparrow, *J. Heat Transfer* **89**, 121 (1967).
- [14] H.-X. Zhou, A. Szabo, J.F. Douglas, and J.B. Hubbard, *J. Chem. Phys.* **100**, 3821 (1994).
- [15] I.C. Kim and S. Torquato, *J. Appl. Phys.* **71**, 2727 (1992).
- [16] T.E. Booth, *J. Comput. Phys.* **39**, 396 (1981).